RSC Advances

ROYAL SOCIETY OF CHEMISTRY

www.rsc.org/advances

Graphical Abstract

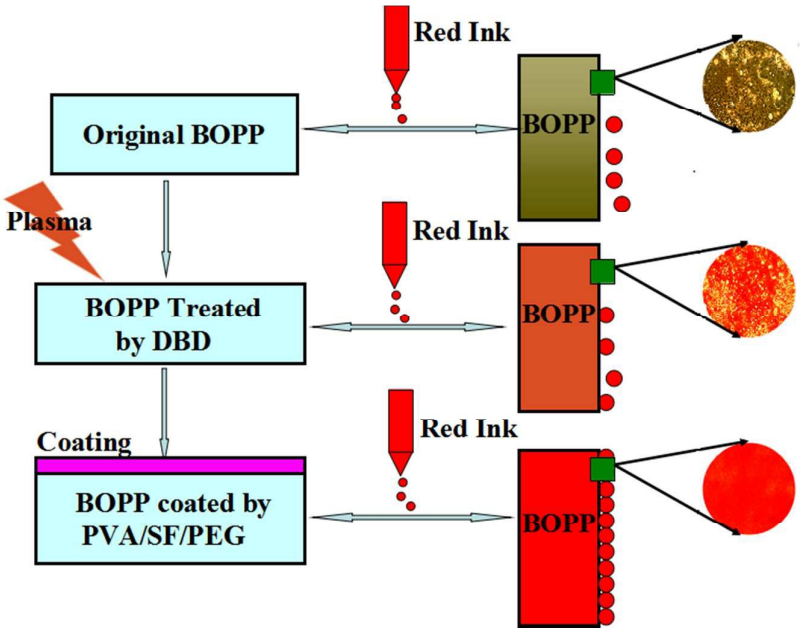

Development of a novel protocol for the permanent hydrophilic modification of a BOPP film for high quality printing with water-based ink

W. X. Chen[a], J. S. Yu[b], G. L. Chen[a1*], X. P. Qiu[a], W. Hu[a], H.Y. Bai[c], J.Z. Shao[a]

[a]Key Laboratory of Advanced Textile Materials and Manufacturing Technology and Engineering Research Center for Eco-Dyeing & Finishing of Textiles, Ministry of Education, Zhejiang Sci-Tech University, Hangzhou 310018, P. R. China

[b]Department of Chemistry and Chemical Engineering, University of New Haven, 300 Boston Post Road, West Haven, CT 06516, USA

[c]The Key Laboratory of Food Colloids and Biotechnology, Ministry of Education, School of Chemical and Material Engineering, Jiangnan University, Wuxi, Jiangsu 214122, P. R. China

Abstract

This paper reports the successful modification of biaxially oriented polypropylene (BOPP) films to permanently enhance their hydrophilic properties for potential flexible packing applications. This protocol consists of three sequential processes: 1) an on-line dielectric barrier discharge (DBD) plasma pretreatment, 2) a polyvinyl alcohol/silk fibroin/polyethylene glycol (PVA/SF/PEG) coating, and 3) ethanol solution finishing. The optimal modification conditions included: DBD plasma pretreatment for 10 seconds, coating with aqueous PVA/SF/PEG (3%/3%/1%) solution, and finally, 8 minutes of treatment with 60% ethanol solution. The fully modified BOPP films exhibited approximately a 16° static contact angle (SCA), a near zero haze value, and an effectively 100% transmittance value under visible light (400–700 nm). The atomic force microscopy (AFM) of the surface morphology of the modified BOPP films showed that the surface roughness increased from 3.79 nm

* To whom the correspondence should be addressed:

Email: glchen@zstu.edu.cn; Tel: +86 571 86843763; Fax: +86 571 86843250

(untreated) to 21.10 nm (fully treated). The Fourier transfer infrared spectroscopy (FT-IR) results showed that polar functional C=O groups were grafted onto the BOPP film that was pretreated with the DBD plasma. Further modification of the pretreated BOPP film with the PVA/SF/PEG coating significantly enhanced the density of the C-O and N-H groups. The gravure printing images indicated that the adhesive property of the BOPP film for water-based ink improved substantially after the hydrophilic modifications.

Keywords: BOPP film; DBD plasma pretreatment; Composite coating; Ethanol solidification; Gravure printing

1. Introduction

Biaxially oriented polypropylene (BOPP) film is widely used in the production of protective coatings, pressure sensitive tape, and decorative products and in labeling and printing [1]. It is also increasingly being used to replace traditional materials such as glass, metal, and paper in food packing applications because it possesses better flexibility, higher transparency, and adequate chemical inertness [2]. However, because of its low surface free energy (SFE) (lower than 22 mJ/m^2 [3, 4]), BOPP film has a low adhesive ability with other materials. Therefore, it is essential to increase the SFE value of the hydrophobic BOPP film to meet the requirements for applications in the material and printing fields. It should be noted that presently the prevailing practice is to use the oily-inks to print on the hydrophobic BOPP films, such practices are unfriendly to both the workers and the environment. Because of the stricter regulations imposed by many countries (both developed and developing countries) on printing industries to minimize environmental concerns, new protocols employing water-based inks for printing are greatly desired and the hydrophilic modification of the BOPP film is therefore of great interest both scientifically and practically.

In recent years, chemical, plasmatic, and corona discharge processes have been applied to increase the SFE value of BOPP film [5]. Among these approaches, the corona discharge technique has gained popularity for industrial applications of BOPP

film because of its simplicity, suitability for continuous online operation, and cost effectiveness. This technique can graft functional groups including hydroxyl, carbonyl, and carboxylic polar groups onto a BOPP film surface, which will increase the SFE value of the modified BOPP film [6]. However, Novak *et al.* [7] showed that the SFE value of corona discharge-treated BOPP film decreases with time.

To mitigate such a drawback, a BOPP film treated by corona discharge with an acrylic acid (AA) monomer was investigated by Liao [8] and Nanticha [6] et al. Unfortunately, the AA polymer coating has a weak water resistance and is generally inhomogeneous because of the filament discharge created by the corona plasma [9]. Additionally, while many vacuum plasma systems have been widely used to modify organic films [10], they are often associated with high operational costs. Therefore, it is necessary to develop a new protocol for the modification of BOPP film, especially for water-based ink printing applications.

In this paper, a novel protocol for the BOPP film modification is reported. The protocol consisted of three sequential processes: 1) the dielectric barrier discharge (DBD) plasma pretreatment, 2) the polyvinyl alcohol/silk fibroin/polyethylene glycol (PVA/SF/PEG) coating, and 3) ethanol solution finishing. The pretreatment of an on-line DBD plasma system ensured an adequate adhesion between the BOPP film and the functional coating, the PVA/SF/PEG coating yielded the desired topology, and the final finishing step with 60% ethanol solution transformed the silk fibroin structure in the functional coating from the alpha helix to beta folding to enhance the hydrophilicity of the modified BOPP film [11].

2. Experimental

2.1 The BOPP film modification system

Fig. 1 illustrates the system employed for the hydrophilic modification of the BOPP film, which consists of four main components: the DBD plasma pretreatment apparatus, the coating device, drying system, and the ethanol treatment chamber. The DBD plasma was realized by using four parallel liquid electrodes, and a quartz tube with a wall thickness of 1 mm acted as the dielectric layer. The gap between the top

and bottom electrodes was 2 mm. An AC power source with a maximum peak voltage of 30 kV and an adjustable frequency range of 8 to 30 KHz was employed for the plasma generation. The discharge power and the treatment time of the plasma system are optimized to 60 watts and 3 s, respectively. The PET pretreatment with DBD plasma can improve the binding intensity between the PET membrane and PVA/SF/PEG film. The PVA/SF/PEG solution warmed in a water tank (40-50°C) was coated homogeneously onto the surface of the pretreated BOPP film using squeeze rollers. Subsequently, the coated BOPP film was dried in the first drying oven (60-80°C) for 120 s. Finally, The PVA/SF/PEG-coated BOPP film passed through the ethanol treatment chamber and was dried by an oven (80-120°C) for 90 s. It should be noted that the batch-type operation can be performed in the step of ethanol processing.

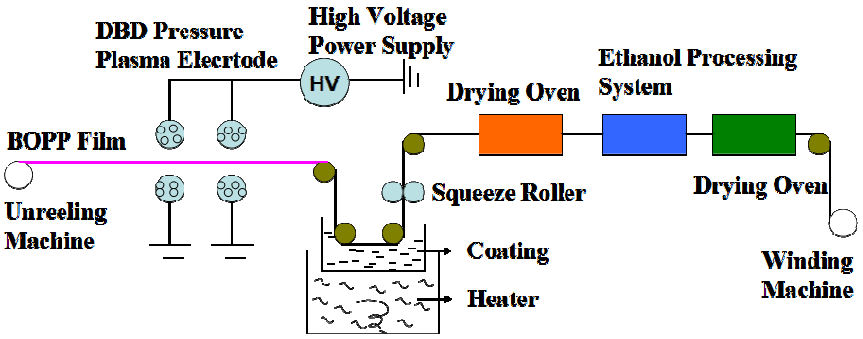

Fig.1. Schematic illustration of the complete system for the BOPP film modification

2.2 Preparation of the PVA/ SF/PEG coating solution

Silk fibroin was obtained following a similar process as reported in our previous work [12]. Briefly, a degummed silk fibroin from B. mori was dissolved in a 9.3 M lithium bromide (LiBr) solution overnight at 37°C, followed by dialysis processing for 3 days to remove the LiBr. PVA (PVA 1797, Shanghai Petrochemical Co., Ltd.) and PEG (PEG 10000, Hangzhou Gaojing Fine Chemical Industry Co., LTD) powders were separately dissolved in deionized water at the desired concentrations (at 80°C and facilitated by a water bath) and mixed with the SF solution at ratios corresponding to the desired SF/PVA/PEG ratios. The rheological characteristic of the PVA/SF/PEG mixture was evaluated using Dynamic Rheometry (Brookfield / DV-III). In this paper,

unless otherwise specified, the PVA, SF, PEG, and ethanol concentrations are all in weight percentages.

2.3 The PVA/SF/PEG coating characterization

Water static contact angle (SCA) measurements (using a Kruss Drop Shape Analysis System (DSA10, Kruss GmbH, Germany)) were employed to characterize the hydrophilicity of the BOPP films that were modified under various conditions. A volume of 3 μL of deionized water was dropped on the surface of the modified BOPP film, and the SCA value was measured with a CCD camera. Three measurements on three different locations of each specimen were performed, and the average SCA value was used for analysis. The surface morphology and roughness of the modified BOPP film was achieved in air under ambient conditions using atomic force microscopy (AFM, XE-100E, PSLA, Korea), which employs a NSC-15/Al probe operated in non-contact mode. Meanwhile, the topography of modified BOPP film was also characterized by a field emission scanning electron microscopy (FESEM, JEOL, Japan). The chemical composition of the modified BOPP film was investigated using XPS (K-Ahpha, USA). The X-ray source was Al Kα at 1486.6 eV and was operated at 300 W. The tensile strength was measured as a representative mechanical property of the modified BOPP film using a tensile strength instrument (XLW-B, Shanghai Tianzhi Co., LTD). The haze and transmittance values of the modified BOPP film were measured with an ultraviolet-visible spectrometer at 633 nm (WGT-S, shanghai Jingke Co., LTD, China). Finally, the gravure printing properties of the modified BOPP film were explored using a pilot-scale roll-to-roll machine (IGT/G1) with a red water-based polyurethane ink (Red-1) (Wuhan Sanhe Surplus Industrial and Trading Company, China).

3. Results and discussion

3.1 The optimal ratio of PVA/SF/PEG for modifying the BOPP film

To determine the optimized PVA/SF/PEG ratio, solutions containing PVA, SF, and PEG at various concentrations were prepared, and the SCA values of the modified BOPP films were measured. Fig. 2 (a) shows the SCA values as a function of the PVA

for various SF and PEG concentrations, and the SCA value initially significantly decreased with an increase in the PVA content. However, the decrease rate became much smaller once the PVA concentration exceeded 3%. In contrast, for the same PVA concentration, the SCA value of the modified BOPP film decreased noticeably with an increase in the SF concentration (lines A to E for 1%, 2%, 4%, 5%, and 6.7%, respectively), with the exception of 3%, which clearly resulted in a significantly lower SCA value, as shown in Fig. 2 (a) for line F. Based on the phenomena observed in Fig. 2 (a) and the effect of the viscosity on the coating process, 3%/3% was selected as the optimized ratio for PVA/SF.

As an excellent softening and dispersant agent, PEG [10] was added to negate the adverse effect (the PVA/SF coating layer was brittle) of the inner stress between the PVA/SF coating and the BOPP film. The experimental results, depicted by line G in Fig. 2 (a), showed that adding 1% of PEG is sufficient for our purposes. The optimized PVA/SF/PEG ratio was determined consequently to be 3%/3%/1%. At this ratio, the SCA value was lower than 20°, which is the desired SCA value for high quality printing in the packing industry. To increase the hydrophilicity of the functional layer, the PVA/SF and PVA/SF/PEG coated BOPP films were further treated with 60% ethanol solution, and Fig. 2 (b) shows the change in the SCA values as a function of treatment time for the samples F and G as shown in Fig. 2 (a) (represented as F* and G*). The data depicted in Fig. 2 (b) indicated that the SCA values of F* and G* as a function of ethanol treatment time followed a “V” pattern and the minimum SCA values of F* and G* lines were approximately 22° and 16°, respectively, with a treatment time of 8 minutes (considered as the optimal ethanol treatment time). Moreover, the treatment with 60% ethanol solution also significantly improved the hydrophilicity of the modified BOPP films (discussed in later sections).

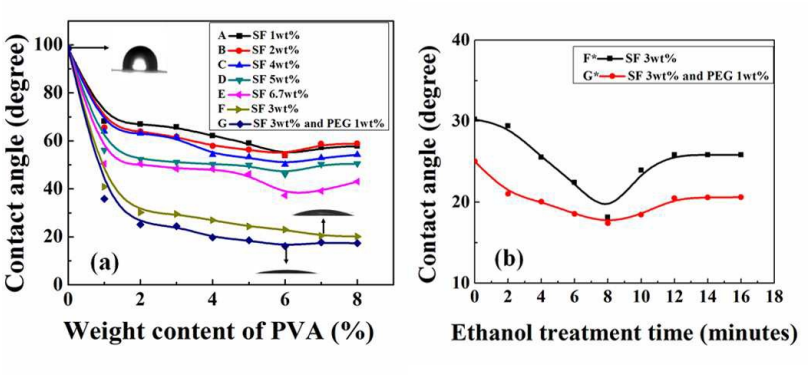

Fig. 2. SCA measurements: (a) The SCA values of the BOPP films modified under various conditions, (b) The SCA values of the BOPP film coated with PVA/SF(F*: 3%/3%) and PVA/SF/PEG (G*: 3%/3%/1%) as a function of the treatment time for the 60% ethanol solution

3.2 The rheological properties of the PVA/SF/PEG solution

The rheological properties of the PVA/SF/PEG solution were evaluated by studying the linear viscoelastic behaviors, as shown in Fig. 3. Figures 3 (a) and 3 (c) show the complex viscosity as a function of the angular frequency. The measured complex viscosity inversely depended on the angular frequency in a near linear manner at low frequencies for two different PVA/SF ratios with/without 1% PEG (3%/3% and 5%/3% for Fig. 3 (a) and 3 (c), respectively). The data depicted in Fig. 3(a) and 3(c) also showed that the measured complex viscosity increased noticeably when the PVA concentration increased from 3% to 5%. Additionally, adding 1% PEG also significantly increased the measured complex viscosity value, which is in good agreement with Zhao [13] and Gahleitner [14].

Figures 3(b) and 3(d) show the values of the storage moduli (lines I and III) and the loss moduli (lines II and IV) as a function of the angular frequency for the samples depicted in Fig. 3(a) and 3(c), respectively. As observed from Fig. 3(b) and 3(d), for both samples, the storage modulus is relatively independent of the angular frequency (lower end), and the addition of 1% PEG would significantly increase the storage modulus and result in an improved elasticity.

However, for the loss modulus and for low angular frequencies, the loss modulus increased with increasing frequency. The addition of 1% PEG resulted in a significant

increase in the loss modulus. However, the data depicted in Fig. 3 (b) showed that such an increase diminished as the frequency increased up to 30 Hz (Line II for no PEG and line IV for 1% PEG, as shown in Fig. 3 (b)). A similar trend for the loss modulus was observed in Fig. 3 (d) as well. However, unlike what was depicted in Fig. 3 (b), the increase in the loss modulus induced by the 1% PEG remained unchanged as a function of frequency until the frequency approached 100 Hz. The phenomena observed in Figs. 3 (b) and 3 (d) indicate that adding 1% PEG increased the flexibility and adhesive property of the functional coating.

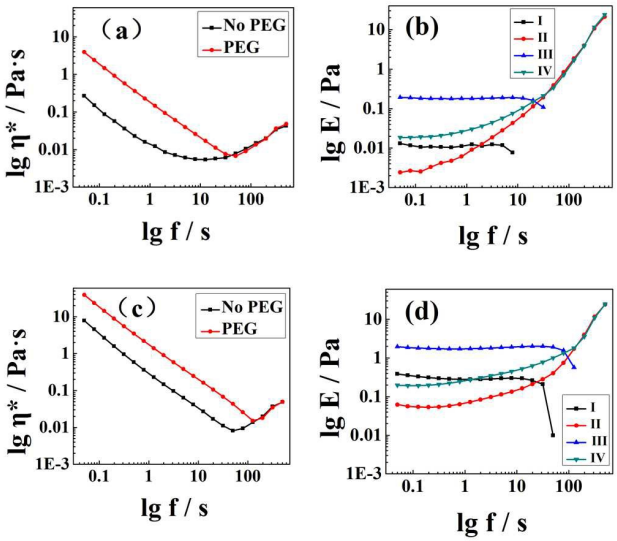

Fig. 3. The rheological behaviors of samples with different PVA/SF/PEG ratios: (a) The PVA/SF (3%/3%) solution, (b) The storage modulus (I without PEG, III with PEG) and the loss modulus (II without PEG, IV with PEG) of the sample (a), (c) The PVA/SF (5%/3%) solution, (d) The storage modulus (I without PEG, III with PEG) and loss modulus (II without PEG, IV with PEG) of the sample (c). The PEG concentration was 1%.

3.3 The mechanical properties of the modified BOPP film

The tensile force (TF_σ, MPa) and the relative elongation (E_ε, %) at break were evaluated to determine the effect of the modification parameters on the mechanical properties of the BOPP film. Table 1 summarizes the relevant mechanical characteristics of the BOPP films modified under various conditions. The thickness, length and width of the original BOPP film were 20 μm, 100 mm and 10 mm,

respectively, and the thicknesses of the PVA/SF/PEG and PVA/SF coating layers were each approximately 1.5 μm. Sample I was the original BOPP film, and its tensile force at break σ (TF_σ) and its elongation at break ε (E_ε) were approximately 138.65 MPa and 9%, respectively. After the DBD plasma pretreatment for 3 seconds (for sample II), the TF_σ and E_ε values increased to 158.7 MPa and 10%, respectively (such increases were considered irrelevant and were usually neglected because of the characteristics of the DBD plasma treatment [15]). The TF_σ and E_ε values of samples III-VIII were compared with those of sample II to identify the effects of the various coating layers. As shown in Table 1, after the BOPP film was modified by the PVA/SF/PEG (of various ratios) coatings, substantial increases in both the TF_σ and E_ε values were observed, and sample VI (PVA/SF/PEG ratio of 3%/3%/1%) exhibited the best mechanical properties in terms of the TF_σ and E_ε values. These observations were consistent with the rheological property analysis in Section 3.2. Moreover, after sample VI was further treated with deionized water or 60% ethanol solution, the TF_σ and E_ε values decreased, but the ethanol solution treatment only marginally decreased. Considering the significant hydrophilicity that was induced by the 60% ethanol solution treatment, such a marginal sacrifice of the mechanical strength was warranted.

Table 1. Mechanical strength properties of the BOPP samples: I: The original BOPP film; II: The DBD plasma pretreated sample; III: The PVA/SF (3%/3%) coated sample; IV: Sample III treated with deionized water for 8 minutes; V: Sample III treated with 60% ethanol solution for 8 minutes; VI: The PVA/SF/PEG (3%/3%/1%) coated sample; VII: Sample VI treated with deionized water for 8 minutes; VIII: Sample VI treated with 60% ethanol solution for 8 minutes

Sample	Tensile force at break σ (MPa)	Elongation at break ε (%)
I	138.65	9.00
II	158.70	10.00
III	215.44	21.00

IV	165.40	16.00
V	210.05	20.00
VI	216.34	26.00
VII	199.05	15.00
VIII	213.32	24.00

3.4 The morphological characteristics of the modified BOPP film

AFM provides both qualitative (visual) and quantitative characterization of the surface morphology of films [16] and was employed in this study. Fig. 4 shows the morphologies and the roughness of the BOPP film treated under different conditions. Compared with the original BOPP film (Fig. 4(a)), the roughness of the BOPP film pretreated by the DBD plasma increased by approximately 90% (from 3.79 to 7.19 nm), and the surface was visually much coarser, as shown in Fig. 4(b). This observation was encouraging because a higher surface roughness often leads to a significantly enhanced combined intensity due to the BOPP film and the functional coating. Fig. 4(c) and 4(d) display the AFM images of the BOPP film modified with PVA/SF (3%/3%) and PVA/SF/PEG (3%/3%/1%) coatings, and a homogeneous distribution of the coating materials is observed in both figures. However, the PVA/SF/PEG coating resulted in a significantly higher roughness of 16.91 nm (a 135% increase from 7.19 nm), whereas only a marginal increase in roughness (from 7.19 to 8.06 nm) was induced by the PVA/SF coating. The addition of 1% PEG was highly beneficial.

Figures 4(e) and 4(f) present the effect of deionized water on the surfaces of the BOPP films that were modified with PVA/SF and PVA/SF/PEG coatings. The treatment with deionized water on the PVA/SF coated BOPP film resulted in a similar topology with a significantly decreased surface roughness (from 8.06 to 3.68 nm, even lower than the 7.19 nm before coating), as shown in Fig. 4(e). However, the treatment with deionized water on the PVA/SF/PEG coated BOPP film resulted in a much different topology with a slightly decreased surface roughness (from 16.91 to 14.07 nm), as shown in Fig. 4 (f). Isolated holes were created, and some had diameters as large as 1 μm. Such a dramatic alteration in the surface topology suggests that the

PEG in the PVA/SF/PEG coating might have leached out into the deionized water. This may be attributed to the high solubility of PEG in water. Fig. 4(f) indicates that a substantial increase in the hydrophilicity of the BOPP film that was coated with the PVA/SF/PEG would be required for it to meet the criteria for high quality printing with water-based ink. This issue was addressed by treating the modified BOPP film with the 60% ethanol solution, as discussed in section 3.1.

Figures 4(g) and 4(h) show the surface morphologies of the PVA/SF and the PVA/SF/PEG coated BOPP film after treatment with the 60% ethanol solution. Some nodules formed due to the ethanol in the PVA/SF coating (see Fig. 4(g)). A potential explanation for this phenomenon is that the contraction of the SF micro-islands during the transformation from the alpha helix to beta folding may extrude the swollen PVA nodules. However, for the PVA/SF/PEG coating, the treatment with 60% ethanol solution still induced the creation of micro holes, but the average depth of these holes was approximately 50 nm, which is substantially lower than those created by the deionized water (approximately 80 nm) (Fig. 4(h) and 4(f)). Moreover, the surface roughness was further increased to 21.10 nm. Such improvements may be due to the restructuring effect of ethanol on the SF, which may have partially reduced the exposure of the PEG content in the PVA/SF/PEG coating.

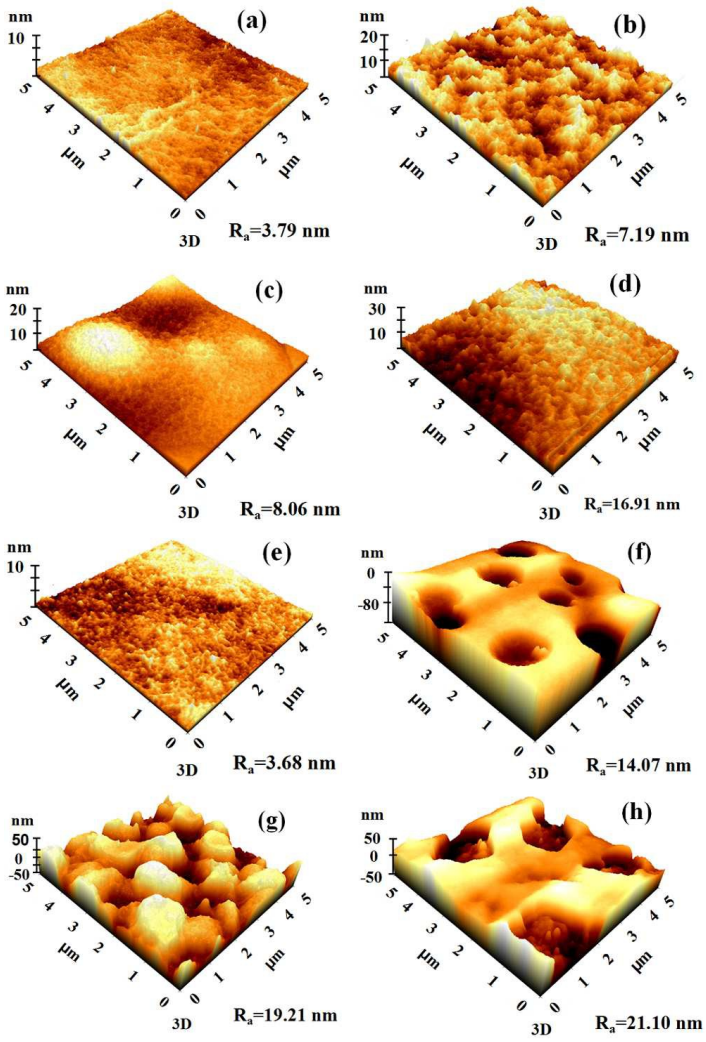

Fig. 4. The AFM 3D images of different samples: (a) The original BOPP film, (b) The BOPP pretreated with DBD plasma, (c) The BOPP pretreated with DBD plasma and coated with PVA/SF (3%/3%), (d) The BOPP pretreated with DBD plasma and coated with PVA/SF/PEG (3%/3%/1%), (e) The sample (c) treated with deionized water, (f) The sample (d) treated with deionized water, (g) The sample (c) treated with 60% ethanol solution, (h) The sample (d) treated with 60% ethanol solution

In order to investigate the effect of processing protocol employed in this study on the BOPP topography, the SEM measurement was also performed. Fig. 5(a) shows the surface morphology of original BOPP film, and it was fairly smooth. After the original BOPP film was treated by the DBD plasma for 3 s, as shown in Fig. 5 (b), many micro-papilla were formed on the BOPP surface and the surface roughness was increased significantly, consistent with the AFM results presented in Fig. 4. When the

plasma pretreated BOPP film was coated with the PVA/SF/PEG coating and dried, as shown in Fig. 5 (c), many micro-islands appeared. A definite mechanism of such an island formation is yet to be determined but it may be caused by the agglomeration of the SF phase in the drying process. Fig. 5 (d) shows the surface of the PVA/SF/PEG coated BOPP film after the 60% ethanol solution treatment. Compared with Fig. 5 (c), the boundary of islands became unclear, which indicates that the phases of PVA and SF in PVA/SF/PEG film were rearranged under the function of ethanol.

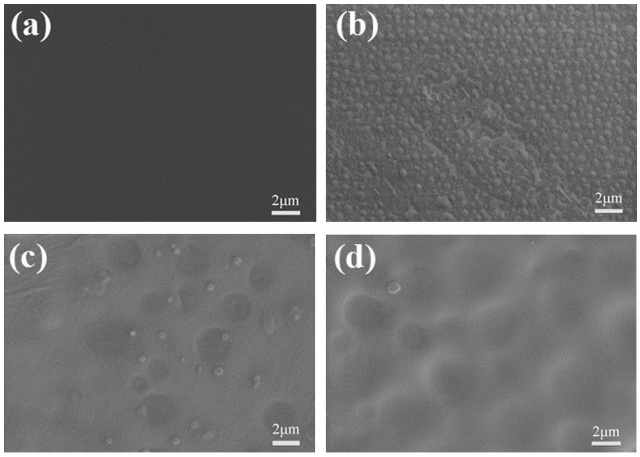

Fig. 5. The SEM images of samples: (a) The original BOPP film, (b) The BOPP pretreated with DBD plasma, (c) The sample (b) coated with PVA/SF/PEG (3%/3%/1%), (d) The sample (c) treated with 60% ethanol solution.

3.5 The chemical structure analysis on the modified BOPP film

A widely used method to probe the chemical constituents of thin films, ATR-FTIR spectroscopy [17], was employed to characterize the chemical structures of the modified BOPP films, as shown in Fig. 6. The assignments of the main absorption peaks in the ATR-FTIR spectra are summarized in Table 2. Curve 1 in Fig. 6 is the spectrum of the original BOPP film. The characteristic peaks at 2930, 1450, 1375, 1168, 978 and 840 cm^{-1} that represent C-H stretching matched well with those previously reported [18-20]. Curve 2 in Fig. 6 is the spectrum of the BOPP film modified with the PVA/SF coating, and new peaks appeared within the range of 1725-1650 cm^{-1}. These new peaks were assigned to the bending of the N-H bond associated with C-N and C-O stretching [21]. When the PVA/SF coated BOPP film was further treated with the 60% ethanol solution, the peak at 1725 cm^{-1} disappeared,

as represented by curve 3. This disappearance may be due to the transformation of the SF [11]. Moreover, the intensity of the absorption bands at 3300 cm^{-1}, which represented the stretching of the N-H or O-H groups, increased substantially, indicating an increased exposure of the PVA or the amide groups to the SF. Curves 4 and 5 in Fig. 6 show the structure conversion of the PVA/SF/PEG coated BOPP film before and after 60% ethanol solution treatment, respectively. All of the absorption peaks decreased. Additionally, the peak at 1080 cm^{-1} in curve 5 also disappeared. The cause for such decreases and the disappearance may be due to possible leaching of the PEG contents into the solution.

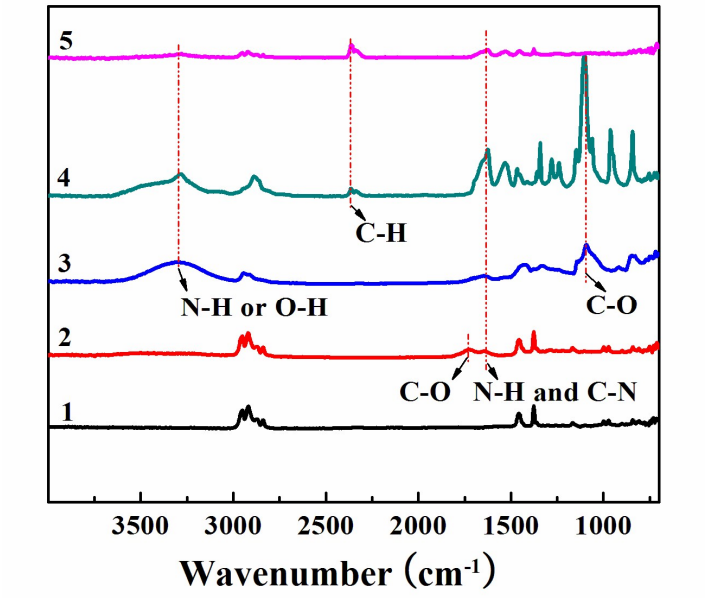

Fig. 6. The ATR-FTIR spectra of the BOPP films: Curve 1: The original BOPP film; Curve 2: The PVA/SF (3%/3%) coated film; Curve 3: Sample 2 treated with 60% ethanol solution; Curve 4: The PVA/SF/PEG (3%/3%/1%) coated film; Curve 5: Sample 4 treated with 60% ethanol solution

Table 2 The assignments of the main absorption peaks in the infrared spectra of the BOPP samples

Absorption Peak/cm^{-1}	Assignment	Vibration type

3300	N-H O-H	Stretching vibration
2930	C-H	Stretching vibration
2350	C-H	Stretching vibration
1725 - 1650	N-H C-N C-O	Stretching and bending vibration
1450 - 1375	CH_2 CH_3	Bending vibration
1100 - 1080	C-O	Stretching vibration

Table 3 summarizes the atomic compositions of the BOPP films, as determined via the XPS analysis. Compared with the original BOPP film (only C was present), 10 seconds of DBD plasma pretreatment exposed O and N and increased the O/C and N/C ratios, indicating the polar groups grafted onto the BOPP surface. These polar groups were beneficial because they increased the adhesive properties of the film surface. Moreover, after the pretreated BOPP film was modified with the PVA/SF/PEG coating, the atomic concentration of O increased significantly and the O/C ratio doubled (compared with the pretreated BOPP film). However, the treatment with 60% ethanol solution resulted in a slightly lower O/C ratio and a substantially higher N/C ratio. This may be due to the bonding of the amino functional groups of the SF on the surface due to the presence of the polar groups in ethanol. Moreover, the treatment with 60% ethanol solution may decrease the surface energy because it increased the surface roughness and the density of the $–NH_2$ groups as the FTIR results presented in Fig. 6. Both lead to lower surface energy, according to the Guimond theory, which suggests that the surface energy of a material is mainly determined by the surface structures and atomic types [22].

Table 3 Summary of the atomic compositions of the BOPP films calculated with the XPS data

Sample	Atomic concentration (%)			Atomic ratio	
	O	N	C	O/C	N/C
Original BOPP film	0	0	100	0	0
DBD pretreated	17.27	2.19	80.54	0.21	0.03

PVA/SF/PEG coated	29	1.9	69.1	0.42	0.03
Ethanol treated (PVA/SF/PEG coated)	25.63	7.64	66.74	0.38	0.11

3.6 The haze and transmittance analysis

The haze and transmittance values are two important parameters for the packing applications of BOPP films. The haze and transmittance values for the original/modified BOPP films are shown in Fig. 7. For the original BOPP film (sample I), the haze and transmittance values were 48.6% and 92.9%, respectively. The DBD plasma pretreatment resulted in a noticeable 21.0% increase in the haze value and a marginal 2.0% decrease in the transmittance value. (sample II in Fig. 7). A significant decrease in the haze value was observed after the BOPP film was modified with the PVA/SF (3%/3%) coating (to 6.4%, as represented by sample III in Fig. 7). Further deionized water treatment led to a lower haze value (2.6%), while further ethanol solution treatment yielded an increased haze value (9%) (samples IV and V, respectively). However, after the BOPP film was modified with the PVA/SF/PEG (3%/3%/1%) coating, the haze value was reduced to near zero, and the transmittance value increased to effectively 100%. Virtually no difference in the haze and transmittance values was observed after the PVA/SF/PEG coated BOPP film was further treated with either deionized water or ethanol solution. The cause of the low haze and high transmittance values was due to the antistatic functional groups [5] and the surface roughness [23, 24].

Lin [25] suggested that a lower surface roughness decreases the haze and increases the transmittance values of BOPP films, in contrary to our results. Our experimental results showed that the BOPP film modified with the PVA/SF/PEG coating had a high surface roughness, a near zero haze value, and a nearly 100% transmittance value. The cause of the discrepancy has yet to be determined but may be due to the hydrophilic nature of the PVA/SF/PEG coating, which generally is associated with reduced haze values [26, 27].

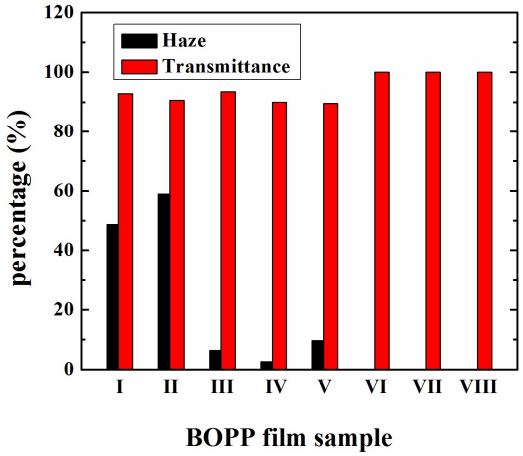

Fig. 7. The visible range haze and transmittance values of the BOPP films: I: The original BOPP film; II: The DBD plasma pretreated film; III: The PVA/SF (3%/3%) coated film; IV: Sample III treated with deionized water; V: Sample III treated with 60% ethanol solution; VI: The PVA/SF/PEG (3%/3%/1%) coated film; VII: Sample VI treated with deionized water; VII: Sample VI treated with 60% ethanol solution

3.7 Printability

Fig. 8 shows the gravure printing quality of the BOPP films that were treated with different methods. The printing quality of the original BOPP film was very poor (multiple ink dots were present), as shown in Fig. 8 (a). The printability increased marginally when the BOPP film was pretreated with the DBD plasma. However, the red ink was still not homogeneously printed on the BOPP surface, as shown in Fig. 8 (b). Fig. 8 (c) demonstrates the printing quality of the BOPP film modified with the PVA/SF/PEG coating, and a substantially higher pixel accuracy was achieved. After further treatment with 60% ethanol solution for 8 minutes, visually flawless printing was achieved, as depicted by Fig. 8 (d). Fig. 8 shows that the novel protocol developed in this study successfully improved the applicability of the BOPP film for high quality printing. Additionally, our experimental results agree with the claim that the wettability is closely associated with the ink adhesion [28, 29].

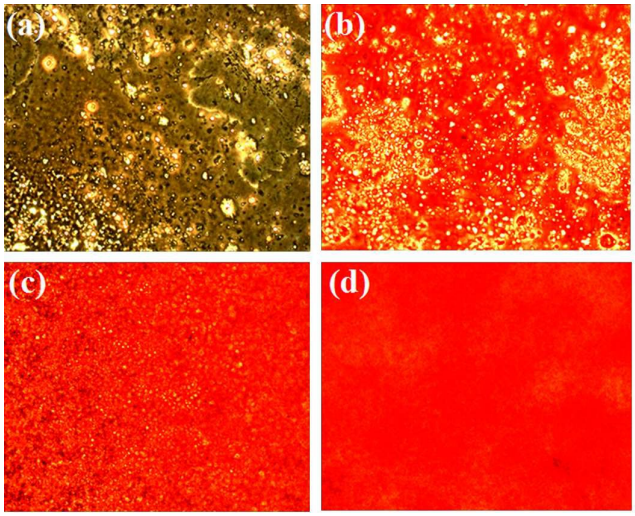

Fig. 8. Images (20 mm x 20 mm) at 100 times magnification of the red water-based ink printed on the BOPP films: (a) On the original BOPP film; (b): On the DBD plasma pretreated film; (c): On the PVA/SF/PEG (3%/3%/1%) coated film; (d): On sample (c) treated with 60% ethanol solution

4. Conclusion

A novel modification protocol was established and an environmentally friendly PVA/SF/PEG coating was designed to improve the printability of BOPP film, making the modified BOPP film highly competitive for packing applications. The entire modification process included DBD plasma pretreatment (corona discharge), PVA/SF/PEG coating, and ethanol solution finishing. The 60% ethanol solution finishing significantly enhanced the hydrophilicity of the BOPP films modified with the PVA/SF/PEG coating. The contact angle of the finished BOPP film decreased from 98.5º to 16.09º after the entire treatment processes, and the haze value decreased to nearly zero, whereas the transmittance value increased to effectively 100%. The surface characteristics of the modified BOPP film are highly competitive for high quality printing applications. Moreover, besides enhancing the printability, the PVA/SF/PEG coating also improved the mechanical strength of the BOPP films. While some micro-holes occurred on the modified BOPP surface, their impact on the printing quality is negligible because the micro-holes are shallow. Indeed, such micro-holes may be favorable because our experimental results indicated that they

may enhance the combined intensity of the ink and the modified BOPP film. High quality printing with water-based ink was achieved using the fully modified BOPP film.

Acknowledgement

We acknowledge support from the National Natural Science Foundation of China under Grant No.11175157, the 521 Talent Project of Zhejiang Sci-Tech University, the Program for Innovative Research Team of Zhejiang Sci-Tech University, and the Young Researchers Foundations of Zhejiang Provincial Top Key Academic Discipline of Chemical Engineering and Technology.

References

[1] Y. W. Wu, C. Y. Han, J. H. Yang, S. X. Jia, S. G. Wang, Surf. Coat. Technol., 2011, **206**, 506–510.

[2] S.K. Pankaj, C. Bueno-Ferrer, N.N. Misra, V. Milosavljevic, C.P. O'Donnell, P. Bourke, K.M. Keener and P.J. Cullen, Trends Food Sci. Technol., 2014, **35**, 5–17.

[3] J.-I. Weon and K.-Y. Choi, Macromol. Res., 2009, **17**, 886-893.

[4] S. Gourianova, N. Willenbacher, M. Kutschera, Langmuir, 2005, **21**, 5429–5438.

[5] B. Nuntapichedkul, S. Tantayanon, K. Laohhasurayotin, Appl. Surf. Sci., 2014, **314**, 331–340.

[6] N. Kalapat, T. Amornsakchai, Surf. Coat. Technol., 2012, **207**, 594–601.

[7] I. Novak, S. Florian, J. Mater. Sci., 2004, **39**, 2033-2036.

[8] J. Lei, X. Liao, Eur. Polym. J., 2001, **37**, 771-779.

[9] X. Zheng, G. L. Chen, Z. X. Zhang, J. Beem, S. Massey, J. F. Huang, Surf. Coat. Technol., 2013, **226**, 123-129.

[10] J. Wu, L. M. Xie, Y. G. Li, H. L. Wang, Y. J. Ouyang, J. Guo, and H. J. Dai, J. Am. Chem. Soc., 2011, **133**, 19668 - 19671.

[11] L. Q. Bai, L. J. Zhu, S. J. Min, L. Liu, Y. R. Cai, J. M. Yao, Appl. Surf. Sci., 2008, **254,** 2988–2995.

[12] G. L. Chen, M. Y. Zhou, Z. X. Zhang, G. H. Lv，Plasma Process. Polym., 2011, **8**, 701–708.

[13] Y. H. Zhao, R. J. Gao, G. Su, H. Lin, C. X. Wang, C. P. Cheng, Mater. Lett., 2013, **91**, 187-190.

[14] M. Gahleitner, Prog. Polym. Sci., 2001, **26**, 895-944.

[15] M. R. Wertheimer, Plasma Chem. Plasma Process., 2014, **34**, 363–376.

[16] G. L. Chen, X. Zheng, J. Huang, X. L. Si, Z. L. Chen, F. Xue and S. Massey, Chin. Phys. B Vol., 2013, **22**, 115206.

[17] Y. Jin, Z. Su, J. Membr. Sci., 2009, **330**, 175–179.

[18] V. Freger, J. Gilron, S. Belfer, J. Membr. Sci., 2002, **209**, 283–292.

[19] A. Prakash Rao, S.V. Joshi, J.J. Trivedi, C.V. Devmurari, V.J. Shah, J. Membr. Sci., 2003, **211**, 13–24.

[20] F. Basarir, E.Y. Choi, S.H. Moon, K.C. Song, T.H. Yoon, J. Membr. Sci., 2005 **260**, 66–74.

[21] Grínia M. Nogueira, Andrea C.D. Rodas, Carlos A.P. Leite, Carlos Giles, Olga Z. Higa, Bronislaw Polakiewicz, Marisa M. Beppu, Bio. Technol., 2010, **101**, 8446–8451.

[22] S. Guimond, I. Radu, G. Czeremuszkin, D. J. Carlsson, and M. R. Wertheimer, Plasmas Polym., 2002, **7**, 71-88.

[23] S. Mangaraj, T. K. Goswami, D. K. Panda, J. Food Sci. Technol., 2014, 1-14.

[24] H. Ashizawa, J.E. Spruiell, J.L. White, Polym. Eng. Sci., 1984, **24**, 1035-1042.

[25] Y.J. Lin, P. Dias, S. Chum, A. Hiltner, E. Baer, Polym. Eng. Sci., 2007, **47**, 1658-1665.

[26] Sh. Rahmatollahpur, T. Tohidi, K. Jamshidi-Ghaleh, J. Mater. Sci., 2010, **45**, 1937-1941.

[27] H. Haidara, Y. Papirer, M. F. Vallat, J. Schultz, J. Mater. Sci., 1993, 28, 3243-3246.

[28] J. W. Lee, K. K. Mun, Y. T. Yoo, Prog. Org. Coat., 2009, **64**, 98-108.

[29] J. W. Lee, Y. T. Yoo, J. Ind. Eng. Chem., 2012, **18**, 1647–1653.